

PAPER • OPEN ACCESS

Effects of Atmospheric Icing on Performance of Controlled Wind Turbine

To cite this article: M Sahin and T Farsadi 2022 *IOP Conf. Ser.: Earth Environ. Sci.* **1121** 012011

View the [article online](#) for updates and enhancements.

You may also like

- [Leading edge topography of blades—a critical review](#)
Robert J K Wood and Ping Lu
- [Effects of Icing on Wind Turbine Fatigue Loads](#)
Peter Frohboese and Andreas Anders
- [Numerical Estimation of Anti-icing Heating Power for NREL 5MW Wind Turbine Blades in Cold Climate](#)
Khaled Yassin, Bernhard Stoesesandt and Joachim Peinke



244th Electrochemical Society Meeting

October 8 – 12, 2023 • Gothenburg, Sweden

50 symposia in electrochemistry & solid state science

Abstract submission deadline:
April 7, 2023

Read the call for papers &
submit your abstract!

Effects of Atmospheric Icing on Performance of Controlled Wind Turbine

M Sahin¹ and T Farsadi²

1 METU Center for Wind Energy Research, Middle East Technical University, Ankara, Turkey

2 Department of Aerospace Engineering, Adana Alparslan Turkes Science and Technology University, Adana, Turkey

E-mail: musahin@metu.edu.tr

Abstract. Icing deteriorates the performance of wind turbine rotors by changing the blade airfoils' shapes. It decreases the lift, increases the drag, and subsequently causes power production losses and load increase on turbines' structures. In the present study, the effects of atmospheric icing on the performance of a controlled large-scale wind turbine is estimated through simulations. To achieve the target, the MS (Mustafa Sahin) Bladed Wind Turbine Simulation Model is used for the analyses of the National Renewable Energy Laboratory (NREL) 5 MW turbine with and without iced blades. Icing modeling is realized based on its main characteristics and its effects on blade aerodynamics. Turbine performance estimations are carried out at various uniform wind speeds between cut-in and cut-out wind speeds and are presented in terms of various turbine parameters such as power, thrust force, blade pitch angle, and rotor speed. Simulation evaluations show that even a light ice accretion along the blades varies the turbine characteristics and dynamics, changes the cut-in and rated wind speeds, and affects the aforementioned turbine parameters differently in the below and above rated regions.

1. Introduction

Wind turbines, which extract the kinetic energy in wind and turn that energy into electrical power, are one of the leading systems for electricity generation and are employed currently in more than 90 countries around the world [1,2].

For wind farm installations, onshore and offshore turbine applications are available. Onshore applications are frequently seen in wind farms, but offshore applications become popular in the last decade, particularly in the last two years [1]. For onshore applications, cold and high-altitude areas are the most convenient sites due to having large wind energy with high-density air and large wind speed [3]. Such sites are available in the Swiss Alps, the northern Scandinavian coastline, China, North America, Canada, etc. [4]. These sites are becoming more important over time as the cost of wind energy drops due to the advances in turbine technology. However, turbines in these regions are exposed to severe atmospheric icing problems during winter seasons [5,6]. In winter, super-cooled water droplets collide with turbine structural surfaces and immediately or after a delay freeze into ice on turbine blades' surfaces.

Icing affects turbine operations in many adverse ways. Accumulated ice on turbine blades changes the blade characteristics and thereby varying the turbine aerodynamics and dynamics. It reduces the turbine aerodynamic performance and causes power losses. It also increases loads on turbines' structures and seriously affects the turbine components such as blades, tower, gearbox, etc. It causes structural fatigue, electrical and mechanical component failures, instrument measurement errors, safety hazards, and so on



[3]. In order to prevent such incidents, for instance, Ref[7,8], previous works of the corresponding author suggests an adaptive algorithm to protect turbines from excessive loads under varying operational conditions as rotor blade icing. In the case of uneven icing on rotor blades, vibrations on the rotor increase, ice particles may detach from the blades, and eventually, the turbine may damage itself and a consequent turbine collapse might be inevitable. Also, operators around turbines may be injured by falling ice deposits. Icing also affects the turbine control system drastically, causing errors in turbine controllers and instrument measurements. For precaution and safety purposes, turbines are often stopped altogether in wind farms [9-11].

Usually, manufacturers consider all of these above situations and produce particular versions of their available turbines for cold region installations. These turbines mostly include anti/de-icing systems (ADIS) for winter operations. As the cost of wind energy has decreased dramatically in recent years, researchers and scientists are focusing more on ice accretion physics to better understand turbine operations in cold places. When ice accretion physics is figured out at certain levels, it allows designers to properly locate the ADIS systems on turbine blades and to design better airfoils or optimize blade airfoils for efficient operation under icing. Also, safety can be increased, Capital Expenditure (CAPEX) and Operational Expenditure (OPEX) may be decreased in an economic sense for the investors [12].

Ice accumulation and thickness on turbine blades increase from root to tip, i.e., less accumulation at the blade root, large accumulation at the tip [9,13,14]. It mainly occurs on the leading edge of turbine blades and linearly increases from root to tip [10]. This decreases the lift and increases the drag of each blade section. Smaller airfoil size and larger effective wind speed towards the blade tip collect more water droplets, resulting in more ice accumulation nearer the tip with larger variation in blade aerodynamics. This study uses the National Renewable Energy Laboratory (NREL) 5 MW turbine to investigate the effects of icing on turbine performance. It is a large-scale turbine with a rotor radius of 63 meters and has a cut-in wind speed of 3 m/s and a cut-out wind speed of 25 m/s [15]. Ice accretion and its effects on the same turbine are numerically studied before by Homola et al. [16] using Blade Element Momentum (BEM) calculations in terms of power output. It is aimed here to show the performance of a controlled large-scale 5 MW turbine with and without icing from cut-in to cut-out wind speed. The performance estimations are given in terms of various turbine parameters such as rotor power, thrust, blade pitch angle and rotor speed since icing and its effects on full turbine behaviour is an area of large uncertainty for both the designers and investors. Turbine simulations are carried out using the MS Bladed Model [2,7,17] at various uniform wind speeds.

2. The MS Bladed Model

The MS (Mustafa Sahin) Bladed Wind Turbine Simulation Model, or the MS Bladed Model [2,7,17] is a Horizontal Axis Wind Turbine (HAWT) simulation tool developed by the first author of this study through the use of MATLAB and Simulink programs. It uses the Blade Element Momentum (BEM) theory along with some important aerodynamic corrections; hub and tip losses, turbulent wake state, and skewed wake rotation. It can simulate large-scale turbines with precone and nacelle/rotor tilt angles, etc., and has similarities to those of Wt_Perf [18] and AeroDyn [19] programs in terms of aerodynamic computations. The MS Bladed Model currently assumes a turbine system to have rigid structures and includes a turbine rotor, a simple variable torque generator, and a gearbox. The dynamic turbine model is given in Equations (1) and (2).

$$J_t \dot{\Omega} = \tau_{aero} - \tau_{gen} \quad (1)$$

$$J_t = J_r + N_{gear}^2 J_{gen} \quad (2)$$

where J_t is the turbine total inertia, Ω is the rotor speed, τ_{aero} is the aerodynamic rotor torque, τ_{gen} is the generator torque on the rotor shaft, whereas J_r is the rotor inertia, J_{gen} is the generator inertia, N_{gear} is the gearbox ratio[2,7,17]. The MS Bladed Model calculates the turbine mechanical power, P and thrust force, T from the following Equations, in which i and j represent, which blade of the turbine and its corresponding blade section, respectively.

$$P = \Omega \sum_i^{B_n} \sum_j^S \frac{1}{2} \rho V_{\text{eff},ij}^2 (Cl_{i,j} \sin \varphi_{i,j} - Cd_{i,j} \cos \varphi_{i,j}) c_{i,j} r_{i,j} \cos \phi_{i,j} dr_{i,j} \quad (3)$$

$$T = \sum_i^{B_n} \sum_j^S \frac{1}{2} \rho V_{\text{eff},ij}^2 (Cl_{i,j} \cos \varphi_{i,j} + Cd_{i,j} \sin \varphi_{i,j}) c_{i,j} \cos \phi_{i,j} dr_{i,j} \quad (4)$$

where B_n is the blade number, S is the number of blade sections, ρ is the air density, V_{eff} is the effective wind speed at a blade section, airfoil Cl and Cd are sectional aerodynamic coefficients, c is the sectional chord length, r is the local radius, ϕ is the rotor precone angle, dr is the sectional length. Effective wind speed, V_{eff} is calculated as follows.

$$V_{\text{eff},ij} = \sqrt{(V_{\text{bx},ij}(1 - a_{i,j}))^2 + (V_{\text{by},ij}(1 + a'_{i,j}))^2} \quad (5)$$

where V_{bx} and V_{by} are freestream velocity components at a blade section, a and a' are axial and tangential induction factors, respectively. Blade pitch angle, β is calculated as,

$$\beta = \beta_p - \beta_T \quad (6)$$

where β_T and β_p are respectively sectional twist angle and the sum of the sectional twist angle and blade pitch angle, β . Turbine efficiency or power coefficient, C_p are calculated by

$$C_p = \frac{P}{\frac{1}{2} \rho (U \cos \theta \cos \Psi)^3 \pi (R \cos \Phi)^2} \quad (7)$$

where U is the wind speed, θ is the rotor tilt angle, Ψ is the turbine yaw angle [17].

3. Baseline turbine controllers

In order to control the NREL 5 MW turbine from cut-in to cut-out wind speed, a generator torque controller and a collective blade pitch controller are designed [7,17]. For the below rated region or Region II, the following standard nonlinear generator torque controller is utilized.

$$\tau_c = K_c \Omega^2 \quad \text{and} \quad K_c = \frac{1}{2} \rho \pi (R \cos \Phi)^5 \frac{C_{p\text{max}}(\lambda_*, \beta_*)}{\lambda_*^3} \quad (8)$$

where τ_c is the torque controller output, Ω is the rotor speed as defined before, K_c is the controller gain, ρ is air density, R is rotor radius, Φ is rotor precone angle, $C_{p\text{max}}$ is maximum power coefficient, whereas λ_* is optimum Tip Speed Ratio or TSR, and β_* is optimum blade pitch angle. Using the MS Bladed Model, λ_* and β_* are obtained respectively as 7.5 and -0.875 degrees. $C_{p\text{max}}$ is determined to be 0.4996. Also, following Ref [15], Region I^{1/2} and Region II^{1/2} transition torque controllers are also designed. The torque actuator dynamics is ignored. The control torque is saturated to 47,402.91 Nm, and a torque limiter of 15,000 Nm/s is added to the generator torque control system [7,17].

For the above rated region or Region III, a gain-scheduled proportional and integral (PI) based collective pitch controller is designed to regulate rotor speed. Pitch to feather control strategy is utilized. The controller gains are scheduled through a gain correction factor as below.

$$\beta(t) = K_p^{\text{GS}} \Delta \Omega(t) + K_i^{\text{GS}} \int \Delta \Omega(t) dt \quad (9)$$

where K_p^{GS} and K_i^{GS} are the gain-scheduled proportional and integral gains, respectively. $\Delta \Omega$ is the rotor speed error between the rotor speed measurement, Ω , and its reference value, Ω_{ref} , whereas β is the pitch controller output. The generator torque is kept fixed at its rated value. Considering Ref [20], the natural

frequency, w_n and damping ratio, ζ are selected as 0.6 and 0.8, respectively. A first-order transfer function with a time constant of 0.2 is used for the pitch actuator dynamics. A rate limiter of 8 deg/s and a saturation limit with a lower bound of -0.875 and an upper bound of +90 degrees are also introduced to the pitch control system[7,17].

4. Icing phenomena and current icing modeling

Icing occurs on turbine blades due to mainly the impingement of super-cooled water droplets to the blade surfaces. The water droplets may freeze on the blade surfaces instantly or after a short delay. Liquid water content, droplet size, temperature, blade surface area, exposure time are the main parameters playing important roles in atmospheric icing. Surface area decides ice accretion rate, whereas water droplet size indicates the type and icing rate [21]. Icing particularly occurs on the leading edge of turbine blades and appears in three types such as rime, glaze, and mixed ice. In a rather cold temperature, i.e., below -10 Celsius, rime ice occurs as soon as the water droplets strike the blade surface with lower liquid water content, low wind speed, and lower median volumetric diameter. Glaze ice is shaped by the water droplets that impinge to the blades and freeze after a delay and occurs in warmer temperatures, i.e., above -10 Celsius with higher liquid water content, high wind speed, and median volumetric diameter. Mixed ice, on the other hand, is a combination of both rime and glaze ice types [5].

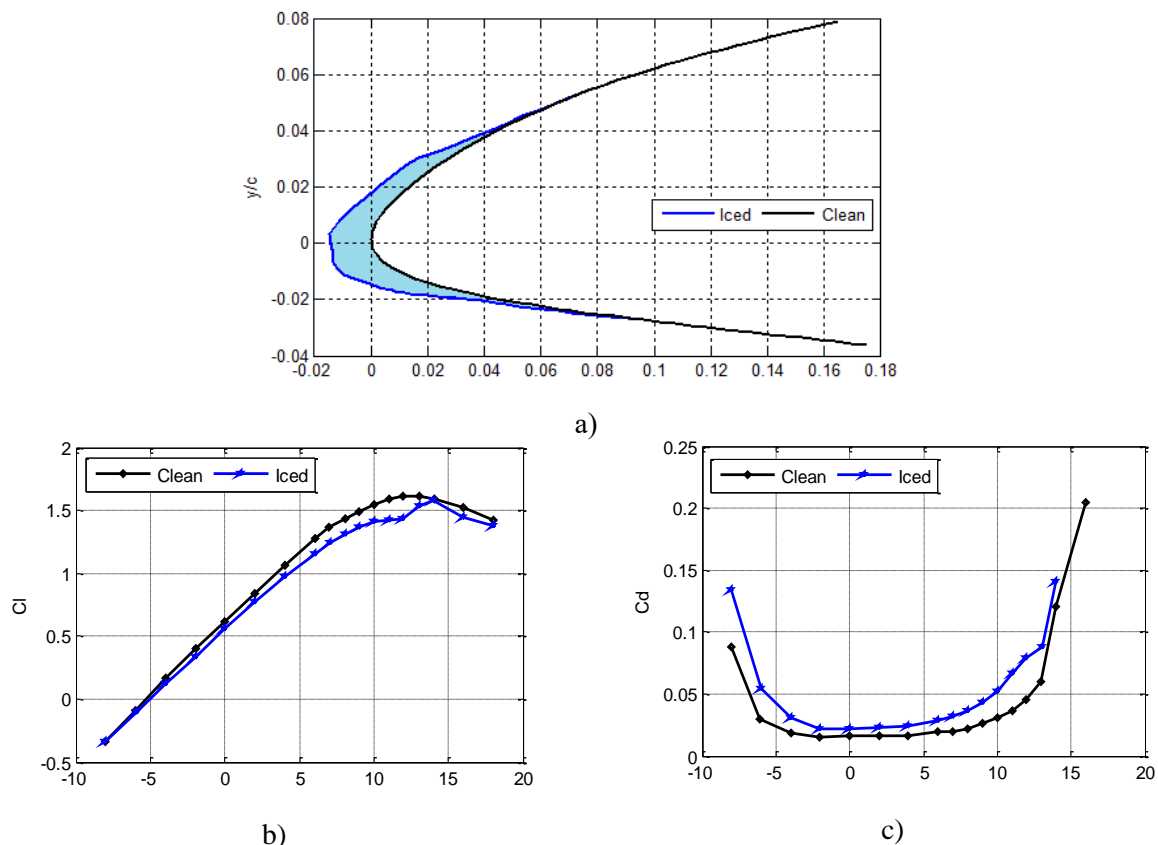


Figure 1. Glaze ice and its effects on blade airfoil aerodynamics of NREL S826, a) Glaze ice, b) C_l data with and without icing, c) C_d data with and without icing [3,8]

For instance, Brandrud and Krøgenes [3] examine these three ice types on a wind turbine blade airfoil, NREL S826, both experimentally and computationally. Using the LEWICE code, they generated ice shapes and conducted various experiments by attaching different artificial ice shapes to the leading edge of the S826 airfoil. Here, for icing modeling, the experimental results of Brandrud and Krøgenes [3] for the glaze icing case are inspired. Figure 1 shows Brandrud and Krøgenes' [3] ice accumulation prediction on the leading edge of the S826 airfoil for the glaze ice type and its resultant effects on C_l and C_d data. To get such an ice shape, they selected the parameters such as freestream icing velocity, V_{icing} ,

temperature, T_{icing} , liquid water content, LWC, mean volume diameter, MVD, icing duration, t_{icing} , angle of attack, AOA, and airfoil chord length, c , as 25 m/s, $-2\text{ }^{\circ}\text{C}$, 0.34 g/m^3 , $30\text{ }\mu\text{m}$, 40 minutes, 1° and 0.3 meters, respectively. By attaching the artificial glaze ice shape (Figure 1-a) to the leading edge of the S826 airfoil, they obtained the experimental Cl and Cd data (Figure 1-b and c) through wind tunnel testing. As seen from Figure 1-a, ice accumulation occurs on the leading edge of the NREL S826 airfoil, and accordingly, it decreases the airfoil lift (Figure 1-b) and increases the drag coefficient (Figure 1-c). Here, such an ice accumulation (Figure 1) is assumed to be accumulated throughout the NREL 5 MW turbine blade span and, by modification, icing effects are introduced to the aerodynamics of turbine blades or Cl and Cd data of blade airfoils. A very light ice accumulation on the blades is taken into account. Even light icing can produce enough surface roughness and significantly reduce the turbine performance, thereby changing its turbine aerodynamic characteristics. Thus, Cl and Cd data of the NREL 5 MW turbine airfoils are slightly modified in this study based on the local blade radius since ice does not accumulate uniformly, increasing from the blade root to tip depending on the blade angular movement. A linear increase in ice accumulation towards the blade tip is considered. As a result, the modification of blade airfoil aerodynamic data increases towards the blade tip, i.e., a slight change in original aerodynamic data at the blade root, a bigger change towards the blade tip. Eventually, imitating the glaze ice formation in Figure 1, the aerodynamic data of all the NREL 5 MW turbine blade airfoils are varied[7,8] and are then used as inputs to the MS Bladed Model. As an example, Figure 2 shows the aerodynamic data of clean and iced DU40A17 and NACA64A17 airfoils of the NREL 5 MW turbine blades, which are located at the 4 and 16th blade sections, respectively.

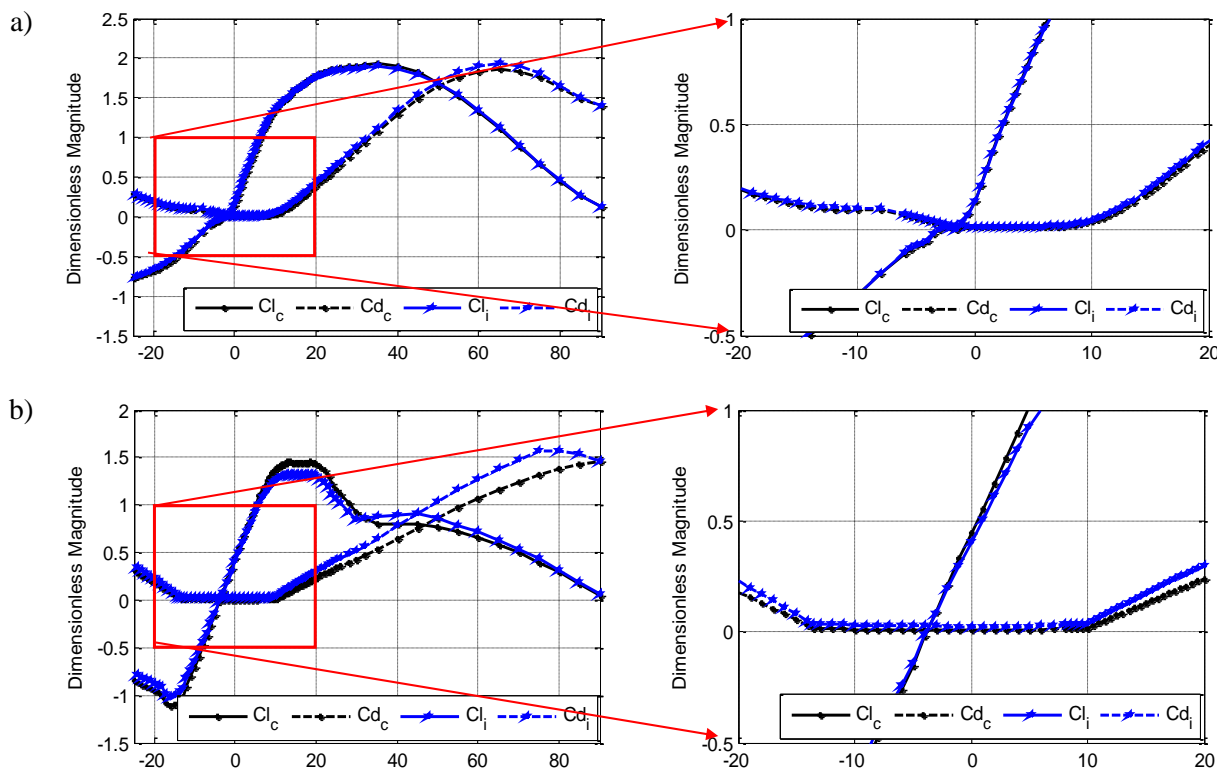


Figure 2. Clean and iced airfoils of NREL 5 MW turbine, a) DU40A17[7], b) NACA64A17

Note that, in Figure 2, Cl_c and Cd_c belong to clean airfoils, while Cl_i and Cd_i belong to iced airfoils. As seen from Figure 2, the change in Cl and Cd are very small for DU40A17 airfoil at the 4th section of the turbine blade, which is close to the root, while the variation in Cl and Cd for NACA64A17 at the 16th section is large close to the blade tip. For all turbine airfoils, from blade root to tip, lift is reduced, while drag is increased to an angle of attack and such that the crossing points of all the lift and drag curves occur around an AOA of 50 degrees, as in the original aerodynamic data, which is a result of

experimental data extrapolation. Here, the modifications are applied to all the NREL 5 MW blade airfoils in between AOA of -25 and 90 degrees. This is because the aerodynamic data of various airfoils particularly differ from each other within this AOA range. Also, both clean and iced airfoil data include the 3D stall delay effect. Lastly, rotor inertia is increased by 3% of the actual inertia due to the considered ice accretion[7,8].

5. Effect of icing on the performance of the NREL 5 MW turbine

In this part, due to ice accumulation considered (Figure 2) on turbine blades, firstly, the NREL 5 MW turbine rotor performance is investigated through the use of MS Bladed Model in terms of power coefficient for cases of clean and iced blades. Later, the steady-state performance estimations of the controlled 5 MW turbine with and without icing are realized at various wind speeds between cut-in and cut-out wind speeds. The MS Bladed simulation results are presented in terms of various turbine parameters such as power, thrust force, blade pitch angle, and rotor speed.

The turbine C_p -TSR curve is obtained by operating the turbine rotor at different TSR values with the blade pitch angle adjusted to the optimum value of -0.875 . Figure 3 shows the C_p -TSR curve of the 5 MW turbine with and without iced blades. Even a very light ice accumulation considered here reduced the turbine efficiency and decreased turbine power coefficient, drastically. At low TSR values, the change in C_p is low, but at high TSR values, the decrease in turbine C_p is quite serious. Throughout all the TSR values, the NREL 5 MW turbine with iced blades has a lower C_p value than the case with clean blades. Due to considered icing, the maximum power coefficient, C_{pmax} of the turbine reduces from 0.4996 to 0.4329. Therefore, there is a 13.35% reduction in C_{pmax} of the 5 MW turbine rotor at the optimum TSR of 7.5.

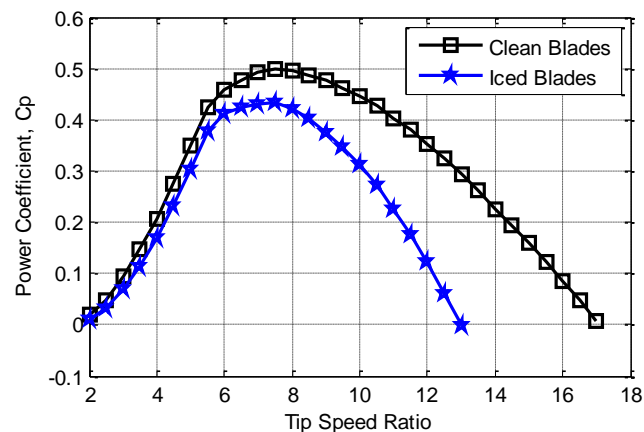


Figure 3. C_p -TSR curve

By applying different uniform wind speeds to the controlled NREL 5 MW turbine with clean and iced blades, the performance estimations are realized using the MS Bladed Model. Performance estimations are presented in Figure 4 in terms of rotor power, thrust force, blade pitch angle, and rotor speed, respectively. The rotor power curve is also compared with the published results of Homola et al. [16]. As seen from Figure 4-a, the 5 MW turbine with iced rotor blades gives a lower power output, compared to that of the clean blades in the below rated region, i.e., Region I^{1/2}, Region II, and Region II^{1/2}. Also, some power loss occurs close to the rated wind speed in the above rated wind speed or Region III. Therefore, for the case with iced blades, the rated power is obtained at a wind speed larger than the actual rated wind speed, i.e., the rated wind speed shifting to a new large value in Region III. However, within the rest of Region III, the turbine produces the rated power, even with iced blades. This is achieved by the collective blade pitch controller. The already-designed blade pitch controller can regulate the turbine rotor speed under the considered icing case.

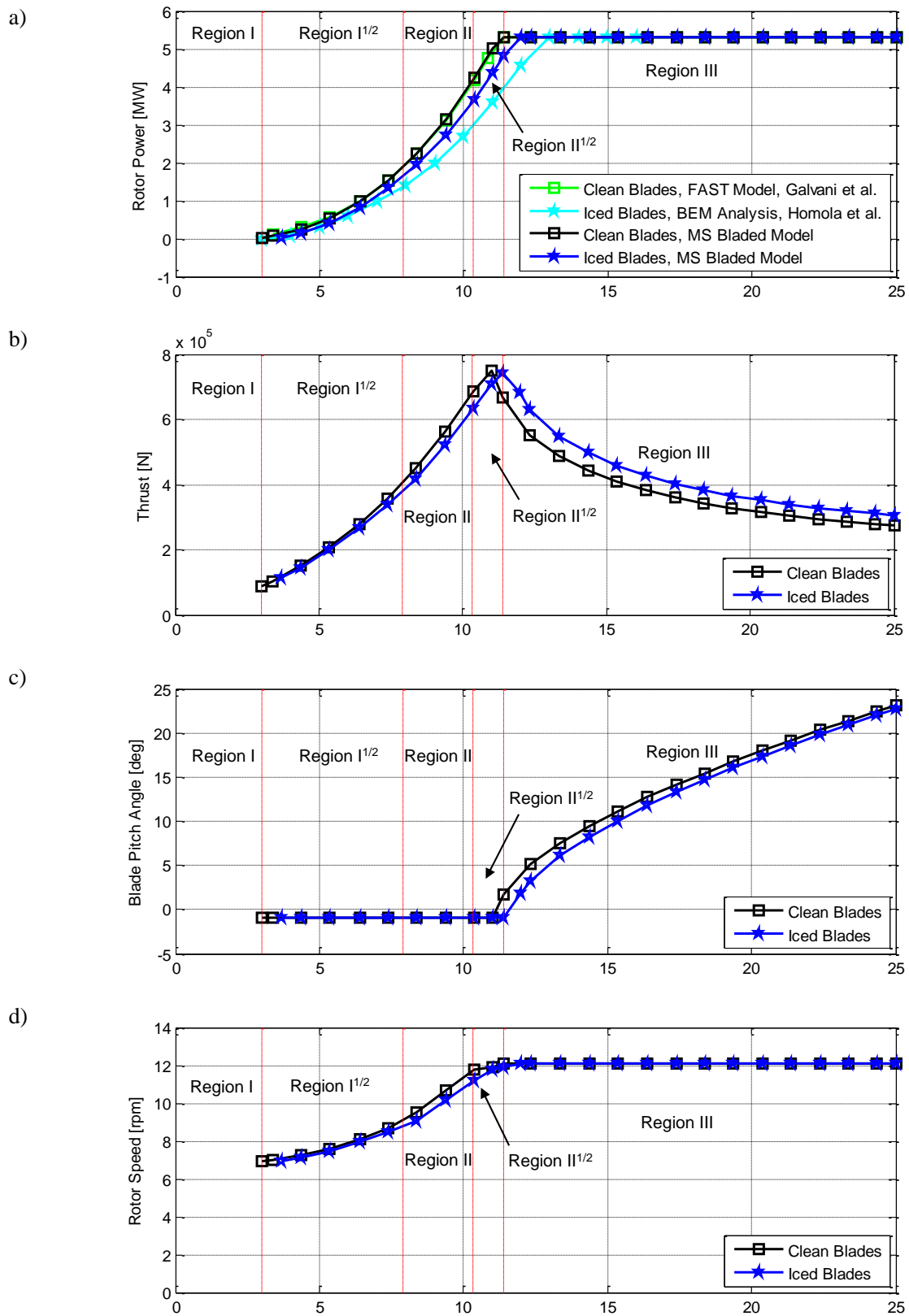


Figure 4. Steady-state performance of the controlled NREL 5 MW turbine, a) Rotor power, b) Thrust, c) Blade pitch angle, d) Rotor speed

The collective blade pitch controller sets the blade pitch angle to lower values than those of the case with clean blades (Figure 4-c). Therefore, it allows the turbine rotor to operate at the rated rotor speed (Figure 4-d) to maintain the rated power in the above rated region (Figure 4-a). On the other hand, the already-designed blade pitch controller still keeps the blade pitch angle at the optimum value of -0.875 degrees both for the cases with clean and iced blades in the below rated region (Figure 4-c). As seen in Figure 4-d, the turbine rotor operates at variable rotor speeds in the below rated region, but with a lower angular speed until the blade pitch controller takes the turbine control in Region III (Figure 4-c). This is an expected rotor speed response because accumulated ice on turbine blades increases the rotor inertia, which is considered to be 3% in this study. Increased rotor inertia varies the turbine dynamics and causes the controlled turbine to reach the steady-state operations at lower rotor angular speeds. It also causes the turbine to start generating electricity at a little higher wind speed in the below-rated region, increasing the cut-in wind speed of the turbine. As a result, the NREL 5 MW turbine starts its operation at 3.7 m/s rather than the actual cut-in wind speed of 3 m/s. Also, the rotor power estimation (Figure 4-a) of Homola et al. [16] using BEM analysis give similar trends as the current simulation results. However, the power losses in the below rated region are much larger than the current case. Also, the rated wind speed is shifted to a much higher value than the value of the actual rated wind speed. All these changes are expected from the amount of ice accumulation on blades and its effects on rotor aerodynamics and inertia. From the simulation results (Figure 4-a), it can be concluded that ice accretion size of Homola et al. [16] on turbine blades is much larger than the currently considered icing in this study.

6. Conclusion

In this study, the effect of icing on the steady-state performance of a controlled large-scale wind turbine is investigated in terms of various turbine parameters such as rotor power, thrust force, blade pitch angle, and rotor speed. A very light ice accretion is considered and icing modeling is realized based on its main characteristics and its effects on blade aerodynamics. The NREL 5 MW turbine is employed for the investigation. For icing modeling, all the airfoil aerodynamic data of the 5 MW turbine are modified based on the blade radius considering a linear ice accumulation throughout the blade span. Simulations with and without iced blades are obtained using the MS Bladed Model. Simulation evaluations show that even a lightly accumulated ice considerably affects turbine rotor performance. It alters the turbine aerodynamics and dynamics. Therefore, it increases the cut-in and rated wind speeds of the controlled turbine. It affects the performance of the controlled turbine differently in different turbine operating regions, i.e., below and above rated regions. The rotor power, rotor speed, and thrust force decrease in the below rated region, whereas the thrust force increases in the above rated region with almost the same power output and rotor speed, but with lower blade pitch settings for the same rated power generation under icing condition.

7. References

- [1] GWEC. (2021). GWEC Global wind report 2021.
- [2] Sahin, M., Yavrucuk, I. (2017). Dynamical modelling of a wind turbine system with precone and tilt angles, 9th Ankara International Aerospace Conference, 1–11, Ankara, Turkey.
- [3] Brandrud, L., Krøgenes, J. (2017). Aerodynamic performance of the NREL S826 airfoil in icing conditions, Master's Thesis, Norwegian University of Science and Technology.
- [4] Barber, S., Wang, Y., Jafari, S., Chokani, N., Abhari, R. S. (2011). The impact of ice formation on wind turbine performance and aerodynamics, *Journal of Solar Energy Engineering, Transactions of the ASME*, 133(1), 1–9, <https://doi.org/10.1115/1.4003187>
- [5] Hu, L., Zhu, X., Chen, J., Shen, X., Du, Z. (2018a). Numerical simulation of rime ice on NREL Phase VI blade, *Journal of Wind Engineering and Industrial Aerodynamics*, 178(May), 57–68, <https://doi.org/10.1016/j.jweia.2018.05.007>
- [6] Parent, O., Ilinca, A. (2011). Anti-icing and de-icing techniques for wind turbines: critical review, *Cold Regions Science and Technology*, 65(1), 88–96, <https://doi.org/10.1016/j.coldregions.2010.01.005>

- [7] Sahin, M., Yavrucuk, I. (2022). Adaptive envelope protection control of wind turbines under varying operational conditions, *Energy*, 247, 123544, <https://doi.org/10.1016/j.energy.2022.123544>.
- [8] Sahin, M., Yavrucuk, I. (2021). An algorithm for wind turbine protection under iced rotor blades, 11th Ankara Intern. Aerospace Conference, AIAC 2021, 8-10 September, 1-12, Ankara, Turkey
- [9] Hochart, C., Fortin, G., Perron, J., Ilinca, A. (2008). Wind turbine performance under icing conditions, *Wind Energy*, 11(4), 319–333, <https://doi.org/10.1002/we.258>
- [10] Shu, L., Liang, J., Hu, Q., Jiang, X., Ren, X., Qiu, G. (2017). Study on small wind turbine icing and its performance, *Cold Regions Science and Technology*, 134, 11–19, <https://doi.org/10.1016/j.coldregions.2016.11.004>
- [11] Ibrahim, G. M., Pope, K., Muzychka, Y. S. (2018). Effects of blade design on ice accretion for horizontal axis wind turbines, *Journal of Wind Engineering and Industrial Aerodynamics*, 173(June 2017), 39–52, <https://doi.org/10.1016/j.jweia.2017.11.024>
- [12] Jin, J. Y., Virk, M. S. (2018). Study of ice accretion along symmetric and asymmetric airfoils, *Journal of Wind Engineering and Industrial Aerodynamics*, 179(June), 240–249. <https://doi.org/10.1016/j.jweia.2018.06.004>
- [13] Hu, L., Zhu, X., Chen, J., Shen, X., Du, Z. (2018b). Numerical simulation of rime ice on NREL Phase VI blade, *Journal of Wind Engineering and Industrial Aerodynamics*, 178(August 2017), 57–68. <https://doi.org/10.1016/j.jweia.2018.05.007>
- [14] Hudecz, A., Koss, H., Hansen, M. O. L. (2013). Ice accretion on wind turbine blades, 15th International Workshop on Atmospheric Icing of Structures (IWAIS XV).
- [15] Jonkman, J., Butterfield, S., Musial, W., Scott, G. (2009). Definition of a 5-MW reference wind turbine for offshore system development, NREL/TP-500-38060, Golden, Colorado: National Renewable Energy Laboratory. Technical Report NREL/TP-500-38060.
- [16] Homola, M. C., Virk, M. S., Nicklasson, P. J., Sundsbø, P. A. (2011). Modelling of ice induced power losses and comparison with observations, 1–13, Winterwind2011.
- [17] Sahin, M. (2018). Dynamic modeling, control and adaptive envelope protection system for horizontal axis wind turbines, PhD Thesis, Department of Aerospace Engineering, METU, Ankara, Turkey.
- [18] Platt, A. D., Buhl, M. L. (2012). WT_Perf user guide for version 3.05.00, Golden, Colorado.
- [19] Moriarty, P. J., Hansen, A. C. (2005). AeroDyn theory manual, NREL/EL-500-36881, Golden, Colorado: National Renewable Energy Laboratory.
- [20] Sahin, M., Yavrucuk, I. (2019). Performance comparison of two turbine blade pitch controller design methods based on equilibrium and frozen wake assumptions, 10th Ankara International Aerospace Conference, AIAC 2019, 1–16, Ankara, Turkey.
- [21] Yirtici, O., Ozgen, S., Tuncer, I. H. (2019). Predictions of ice formations on wind turbine blades and power production losses due to icing, *Wind Energy*, 22(7), 945–958. <https://doi.org/10.1002/we.2333>